Carbohydrate Research 464 (2018) 12–18

Contents lists available at ScienceDirect

Carbohydrate Research

journal homepage: www.elsevier.com/locate/carres

An anticoagulant fucan sulfate with hexasaccharide repeating units from the sea cucumber *Holothuria albiventer*

Ying Cai[a,b], Wenjiao Yang[a,b], Ronghua Yin[a,b], Lutan Zhou[a], Zhongkun Li[c,*], Mingyi Wu[a,*], Jinhua Zhao[a,*]

[a] State Key Laboratory of Phytochemistry and Plant Resources in West China, Kunming Institute of Botany, Chinese Academy of Sciences, Kunming, 650201, China
[b] University of Chinese Academy of Sciences, Beijing, 100049, China
[c] Department of Pharmacy, Yan'an Hospital Affiliated to Kunming Medical University, Kunming, 650051, China

ARTICLE INFO

Keywords:
Fucan sulfate
Chemical structure
Anticoagulant
Polysaccharide
Sea cucumber

ABSTRACT

A fucan sulfate was isolated and purified from the sea cucumber *Holothuria albiventer* by papain enzymolysis, alkaline hydrolysis and ion-exchange chromatography. The water-soluble polysaccharide had high molecular weight and contained fucose and sulfate in a molar ratio of about 1:0.83. Methylation analysis of the native polysaccharide indicated that its glycosidic linkages and sulfate substituents might be at *O*-3 or *O*-3, 4 or *O*-2, 3, or *O*-2, 3, 4 positions. FT-IR and 2D NMR spectroscopies further revealed that the fucan sulfate is characteristically composed of a regular α (1 → 3) linked hexasaccharide repeating unit which is substituted with sulfate esters in a distinctive pattern. Anticoagulant properties of the fucan sulfate and its depolymerized product were assessed *in vitro* in comparison with a low-molecular-weight heparin. The fucan sulfate exhibits strong APTT and TT prolonging activities and intrinsic factor Xase inhibitory activity, and its molecular size seemed to be required for these activities.

1. Introduction

Unfractionated heparin (UFH) and low-molecular-weight heparins (LMWHs) have been the cornerstones of antithrombotic treatment and prophylaxis for the last 70 years, which are the only type of sulfated polysaccharide currently used as anticoagulant drugs [1,2]. The commercial sources of heparins are mainly porcine intestinal mucosa and bovine lung, where the heparin content is low [3]. The possibility that concomitants such as prions and viruses may be carried by the biological products combined with the increasing demand for antithrombotic therapies indicates the necessity to research for alternative sources of anticoagulant agents [4].

Marine echinoderm and brown alga are abundant sources of anticoagulant polysaccharides, such as fucoidans and fucan sulfates [4–17]. Brown algal polysaccharides, called fucoidans, usually are mixtures of several sulfated polymers with complex monosaccharide composition, thus they are structurally non-regular and heterogeneous [4–10], which hinders the clarification of their structure-activity relationship [10,11]. Distinguishing from fucoidans, the fucans from echinoderm such as sea cucumber and sea urchin, often known as fucan sulfates (FSs), are structurally more regular for they comprise only one kind of monosaccharide [12–18]. The chemical structures of these fucan sulfates were found to be species-specific [12,17]. Thus, each new sulfated polysaccharide purified from a certain sea cucumber or sea urchin would be a new compound with unique structures and, consequently, with potential novel biological activities.

Recently, when searching for new anticoagulant sulfated polysaccharides, we obtained two fucan sulfates from two species of sea cucumbers *Holothuria edulis* and *Ludwigothurea grisea* [16,17]. Both fucan sulfates have a unique structure composed of a central core of regular (1 → 2) and (1 → 3)-linked tetrasaccharide repeating units. Approximately 50% units of the FS from *L. grisea* (100% for *H. edulis* FS) contain side chains that are formed by nonsulfated fucose residues and linked to the *O*-4 positions of the central core. Anticoagulant activity assays indicated that the sea cucumber FSs can strongly inhibit human blood clotting through the intrinsic pathway of the coagulation cascade. Their distinctive structure with the tetrasaccharide repeating units contributes to the anticoagulant action [17].

Further exploration of sulfated polysaccharides from other sea cucumber species would provide a wider insight into the studies on their chemical structures and functional activities. In the present study, we discovered a new fucan sulfate from the sea cucumber *Holothuria albiventer*. The chemical structure was analyzed by chemical and instrumental methods such as Fourier transform infrared spectroscopy

* Corresponding authors.
E-mail addresses: yayylzk@163.com (Z. Li), wumingyi@mail.kib.ac.cn (M. Wu), zhaojinhua@mail.kib.ac.cn (J. Zhao).

https://doi.org/10.1016/j.carres.2018.05.007
Received 31 March 2018; Received in revised form 15 May 2018; Accepted 17 May 2018
Available online 19 May 2018
0008-6215/

Table 1
GC–MS of alditol acetate derivatives from the methylated product of the fucan sulfate from the sea cucumber *H. albiventer*.

Methylated Derivatives (as alditol acetates)[a]	Positions of substitution	Relative retention time[b]	Molar ratio	Primary mass fragments (m/z)
2, 4-Me_2-Fuc	3	1.00	1.00	89, 101, 117, 131,159, 173, 233
2-Me-Fuc	3, 4	1.14	0.51	87, 99, 117, 129, 173, 275
4-Me-Fuc	2, 3	1.22	0.79	89, 99, 131, 159, 201, 261
Fuc	2, 3, 4	1.35	5.60	115, 128, 145, 170, 217, 231, 289

[a] 2, 4-Me_2-Fuc: 1,3,5-tri-*O*-acetyl-2,4-di-*O*-methyl-*L*-fucitol; 2-Me-Fuc: 1, 3, 4, 5-tetra-*O*-acetyl-2-*O*-methyl-*L*-fucitol; 4-Me-Fuc: 1,2,3,5-tetra-*O*-acetyl-4-*O*-methyl-*L*-fucitol; Fuc: 1,2,3,4,5-penta-*O*-acetyl-*L*-fucitol.

[b] Relative retention times of the corresponding alditol acetate derivatives compared to 1,3,5-tri-*O*-acetyl-2,4-di-*O*-methyl-*L*-fucitol.

(FT − IR), high performance liquid chromatography (HPLC), monosaccharide composition analysis, and nuclear magnetic resonance (NMR) spectroscopies (1D ^{1}H, ^{13}C, 2D ^{1}H/^{1}H COSY, TOCSY, ROESY, 2D^{13}C/^{1}H HSQC and HMBC). Moreover, its effect on the clotting time of human plasma and intrinsic coagulation factor Xase complex were investigated. Our results may provide valuable information for understanding the structure-function relationships of the well-defined polysaccharides from invertebrate.

2. Results and discussion

2.1. Purification and physicochemical characterization

The body wall of sea cucumber usually contains two types of sulfated polysaccharides, fucosylated chondroitin sulfate and fucan sulfate [16–19]. The crude polysaccharides, with the yield of about 8.0% by dry weight, were extracted from the sea cucumber *H. albiventer* by the papain enzymolysis and alkaline hydrolysis [16]. The fucosylated chondroitin sulfate was partially removed by ethanol precipitation and KOAc salting out [19,20]. Then the crude fucan sulfate was further purified into different fractions by anion exchange chromatography using a FPA98 column. The fucan sulfate fraction obtained from the sea cucumber seemed to display high purity as determined by the high-performance gel permeation chromatography (HPGPC) (Figure S1). Ultraviolet absorption at around 260 or 280 nm was not observed as detected by an UV-detector, indicating the absence of contaminants of protein or peptides.

Additionally, the HPGPC profile of the fucan sulfate displayed a single wide peak, indicating that the polysaccharide might be homogenous with a wide distribution. And its average molecular weight was over 2000 kDa as calculated by GPC. The monosaccharide composition of the sea cucumber polysaccharide was qualitatively identified by reverse-phase HPLC after PMP derivatization procedures [21,22]. The result showed that the fucan sulfate contained the only monosaccharide fucose, which consists with those from other sea cucumber species [15,16,18] (Figure S2). The specific rotations of the polysaccharide and its depolymerized product were −168° and −172°, respectively, similar to those from other sea cucumber species [16,17]. This result is in conformity with *L*-configuration of fucose residues [17,23].

Among other diagnostic information, the content of possible charged groups, such as sulfate groups, is essential to evaluate the charge distribution along the polyelectrolyte chain. Thus, the charge of the native fucan sulfate and its depolymerized product was measured by conductometric titration [24]. Both of conductimetric titration curves showed only one inflection point (Figure S3), indicating that the fucan sulfate contains only a negatively charged functional group. Further calculation indicated that the sulfate (SO_4) content of the native fucan sulfate was 34.4% (37.9% for the depolymerized fucan sulfate), and the molar ratio of sulfate ester to monosaccharide was 0.83 (0.93 for the depolymerized fucan sulfate).

To analyze the positions of its glycosidic linkages and sulfate ester substituents in the fucan sulfate, methylation and GC-MS analysis was carried out by the previous method [17,21,25]. Consequently, the four monosaccharide derivatives identified by MS analysis were 1,3,5-tri-*O*-acetyl-2,4-di-*O*-methyl-*L*-fucitol (2, 4-Me_2-Fuc), 1,3,4,5-tetra-*O*-acetyl-2-*O*-methyl-*L*-fucitol (2-Me-Fuc), 1,2,3,5-tetra-*O*-acetyl-4-*O*-methyl- *L*-fucitol (4-Me-Fuc), and 1,2,3,4,5-penta-*O*-acetyl-*L*-fucitol (Fuc) with a molar ratio of 1.00: 0.51: 0.79: 5.60 as calculated by their peak areas, respectively (Table 1). The result suggested that its glycosidic linkages and sulfate substituents might be at *O*-3 or *O*-3, 4 or *O*-2, 3, or *O*-2, 3, 4 positions of fucose residues in the polymer chains. Since the four substituents were all at *O*-3 positions, we inferred that the fucan sulfate might consist of (1 → 3) linked fucose residues sequences. Other techniques such as NMR analysis of its desulfated product would further confirm the $[(1 \rightarrow 3)\text{-Fuc}]_n$ backbone in a structure of the fucan sulfate (see the following results).

2.2. IR and NMR analysis

The organic functional groups of the *H. albiventer* fucan sulfate were further characterized by IR spectroscopy (Figure S4A). The bands in the region of 4000–1800 cm^{-1} showed the characteristic O–H and C–H stretching vibrations of this polysaccharide at 3442 cm^{-1} and 2942 cm^{-1}, respectively [26]. Three signal groups were assigned to the sulfate groups, particularly, those appeared at 1262 and 1231 cm^{-1} were caused by S = O asymmetric stretching vibration, that at 854 cm^{-1} were assigned to the symmetric C–O–S stretching vibration and that at 583 cm^{-1} were caused by S–O stretching vibration [26–28]. These data confirmed that the sea cucumber polysaccharide was substituted by sulfate esters. Carbohydrate signals in the 1500–1200 cm^{-1} region indicated the deformation vibrations of H–C–H, C–O–H, C–H and C–O–C groups. Bands in this region at 1453 cm^{-1} and 1384 cm^{-1} may be assigned to the asymmetric and symmetric deformation vibrations of CH_3, respectively. These bands were also observed in the second-derivative spectrum of fucoidan [29]. In the finger print region, band at 962 cm^{-1} was assigned to the asymmetric and symmetric deformation vibrations of the methenyl groups in fucose residues [27]. The FT-IR spectrum of the depolymerized fucan sulfate (Figure S4B) was similar to that of the native fucan sulfate, implying their structural group similarity.

The 1D ^{1}H NMR spectrum of the fucan sulfate displayed overlapping and broad signals with line widths of several Hz (Figure S5), owing to its highly polymeric nature as high-molecular-weight compound, which hampered the resolution. It would be useful to study the desulfated product of the native sulfated polysaccharide to clarify the glycosidic linkages of its backbone. The sulfate content (Figure S3C) and the molar rate of sulfate ester to fucose of the desulfated product were 15.6% and 0.28, respectively, and the desulfation rate was about 70% compared to the native fucan sulfate. Minor signals at about 5.3 ppm in the ^{1}H NMR spectrum of the soluble desulfated product might indicate incomplete desulfation (Figure S6). The molecular weight of the desulfated product was 1638 Da. The result indicated that the fucan sulfate may be excessively degraded under desulfation conditions. Degradation of other fucan sulfates was also observed previously in the desulfation procedure [30,31]. Nevertheless, the 1D NMR spectra of the desulfated product (Figure S6) indeed became simpler than those of the native sulfated polysaccharide. The chemical shifts of individual residues in the desulfated product were fully assigned (Table S1) according to 1D (^{1}H, ^{13}C) and 2D ^{1}H/^{1}H COSY, TOCSY, ROESY, 2D^{13}C/^{1}H HSQC, and

Table 2
$^{1}H/^{13}C$ NMR chemical shift assignments of the depolymerized fucan sulfate from the sea cucumber *H. albiventer*.

	residues	A	B	C	D	E	F
^{1}H	**H1**	5.379/5.340	5.346/5.310	5.012	5.306/5.284	5.046	5.035
δ (ppm)	**H2**	**4.426**[a]**/4.460**	**4.519**	3.876	**4.499**	3.795	3.766
	H3	*4.203*[b]*/4.236*	*4.344/4.311*	*3.939/3.873*	*4.061*	*3.885*	*3.943*
	H4	**4.757/4.741**	**4.861/4.851**	3.898/**4.233**	4.032	3.957	3.975
	H5	4.362	4.366	4.386	4.261	4.246	4.483
	H6	1.188	1.195	1.208	1.192	1.188	1.216
^{13}C	**C1**	100.47/97.83	96.63/96.38	97.69/97.65	97.65/95.84	100.75	102.0/101.8
δ (ppm)	**C2**	**75.25**	**77.21**	68.78	**75.33**	69.05	69.01
	C3	*76.8*	*76.37/75.66*	*78.31/78.46*	*76.63*	*76.85*	*78.07*
	C4	**82.41/82.21**	**82.97**	70.69/**77.27**	71.75	71.06	70.85
	C5	69.80	69.20	69.55	68.69	68.69	68.95
	C6	17.89	18.14	17.65/17.46	17.58	17.79	18.00

[a] Values in bold type indicate the positions of sulfation.
[b] Values in italic type indicate the glycosylated positions.

HSQC-TOCSY spectra (Figure S6). The correlation peaks in 2D $^{1}H/^{1}H$ ROESY and $^{13}C/^{1}H$ HSQC-TOCSY spectra (Figure S6E, G) confirmed the $[(1\rightarrow3)\text{-Fuc}]_n$ backbone in a structure of the fucan sulfate (Figure S7).

To further elucidate the structures in detail, its low-molecular-weight depolymerized product was obtained by our previously established radical depolymerization method [26]. The chemical shifts of individual residues in the depolymerized product were fully assigned (Table 2) according to 1D (^{1}H, ^{13}C) (Fig. 1, Figure S8) and 2D $^{1}H/^{1}H$ COSY, TOCSY, ROESY, 2D$^{13}C/^{1}H$ HSQC, and HMBC experiments (Fig. 2).

In the 1D ^{1}H NMR spectrum of the depolymerized fucan sulfate (Figure S8A), strong signals observed at around 1.1–1.2 ppm were the characteristic signals of methyl protons in the *L*-fucose residues [17,18]. Notably, six main signals at 5.0–5.5 ppm could be unambiguously observed in the 1D ^{1}H NMR spectrum (Fig. 1A), which were attributed to the anomeric resonances of α-fucopyranosyl residues with different sulfation patterns [16–18,32]. Further, 2D $^{1}H/^{1}H$ COSY spectrum (Fig. 2A) clearly showed six spin-coupled systems (**A**, **B**, **C**, **D**, **E**, **F**) and the six types of residues showed roughly equal integral areas in the 1D ^{1}H NMR spectrum, indicating that the fucan sulfate might be composed of hexasaccharide repeating units. To assign other proton signals in the spectra, 2D $^{1}H/^{1}H$ COSY and TOCSY NMR analyses were employed to complete these proton assignments (Fig. 2A and B). Starting from their anomeric protons, some protons from six spin systems were identified in the 2D $^{1}H/^{1}H$ COSY spectrum. According to the correlation peaks in the 2D $^{1}H/^{1}H$ TOCSY spectrum, the proton chemical shifts could further be well assigned as shown in Fig. 1A and Table 2. The *H*-2 shift values of **A**, **B**, and **D** residues in the fucan sulfate at 4.4–4.5 ppm was shifted downfield by about 0.6 ppm compared with those of non-sulfated fucose residues [17,20,32,33], indicating the sulfation substitution at *O*-2 of these residues. Likewise, the *H*-4 shift values of **A**, **B**, and **C** residues indicated that the fucan sulfate may possess 4-*O*-sulfated fucose residues. The *O*-4 positions of **C** residues were partly sulfated, and the non-sulfated **C** residues accounted for about 70% (in mole), which may contribute to the complexity of its chemical structure. And for the C residues with partially sulfated *O*-4 positions may have certain effect on the $^{1}H/^{13}C$ chemical shifts of other residues such as residues A, B and D, two sets of the NMR signals for the units A, B and D were thus observed here (Table 2).

Additionally, the chemical shifts values of all carbons in the depolymerized fucan sulfate were assigned according to the 1D^{13}C and 2D$^{13}C/^{1}H$ HSQC spectra (Fig. 1B, Figure S8B, Fig. 2D) and presented in Table 2. In the 1D^{13}C NMR spectrum of the depolymerized fucan sulfate, the signals at 102–96 ppm were produced by the anomeric carbons (*C*-1). The strong signals occurred at ~18 ppm could be assigned to the methyl groups (*C*-6) [17,18,20]. Owing to the reference to trimethylsilyl-propionic sodium salt, chemical shifts of ^{13}C nuclei generally do not completely agree with our earlier related publication [17]. The downfield chemical shifts of *C*-2 of the **A**, **B** and **D** residues and *C*-4 of the **A**, **B** and **C** residues further confirmed their respective sulfated substitution positions, consistent with the proton chemical shifts analysis (values in boldface indicate the positions bearing sulfate groups as shown in Table 2).

Furthermore, structural features of the fucan sulfate including the glycosidic linkages and the residue sequences were confirmed according to the correlation peaks in 2D $^{1}H/^{1}H$ ROESY and $^{13}C/^{1}H$ HMBC spectra (Fig. 2C, E). The correlation between H-1 and H-3 of these residues was identified in the 2D $^{1}H/^{1}H$ ROESY spectrum (Fig. 2C), confirming the presence of $(1\rightarrow3)$ linkages in the fucan sulfate. The sequences of these repeating units were also confirmed by the long range scalar correlations in the 2D$^{13}C/^{1}H$ HMBC spectrum (Fig. 2E).

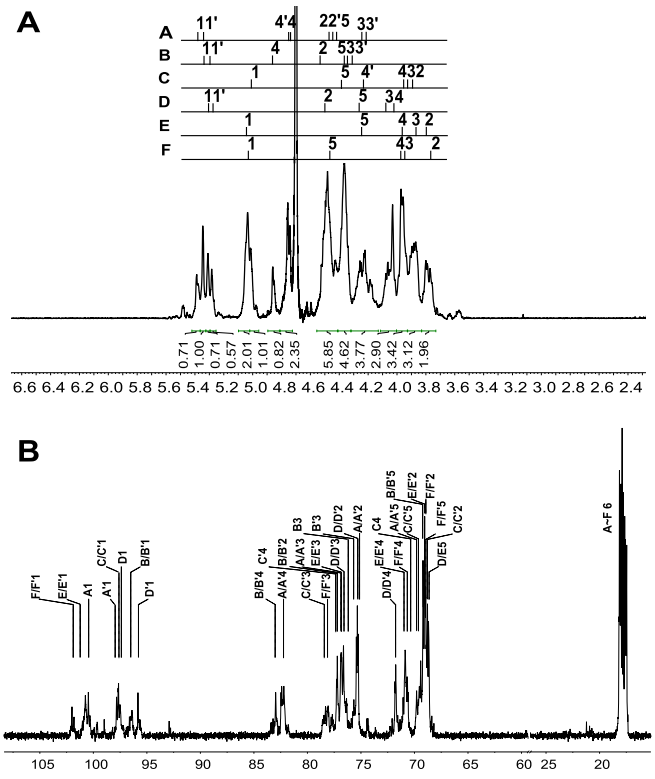

Fig. 1. ^{1}H (**A**) and ^{13}C (**B**) NMR spectra of the depolymerized fucan sulfate with molecular weight of ~4 kDa. Chemical shifts are relative to the external trimethylsilylpropionic acid at 0 ppm in the ^{1}H and ^{13}C spectra, respectively. The numbers following the letters indicate the positions of ^{1}H and ^{13}C.

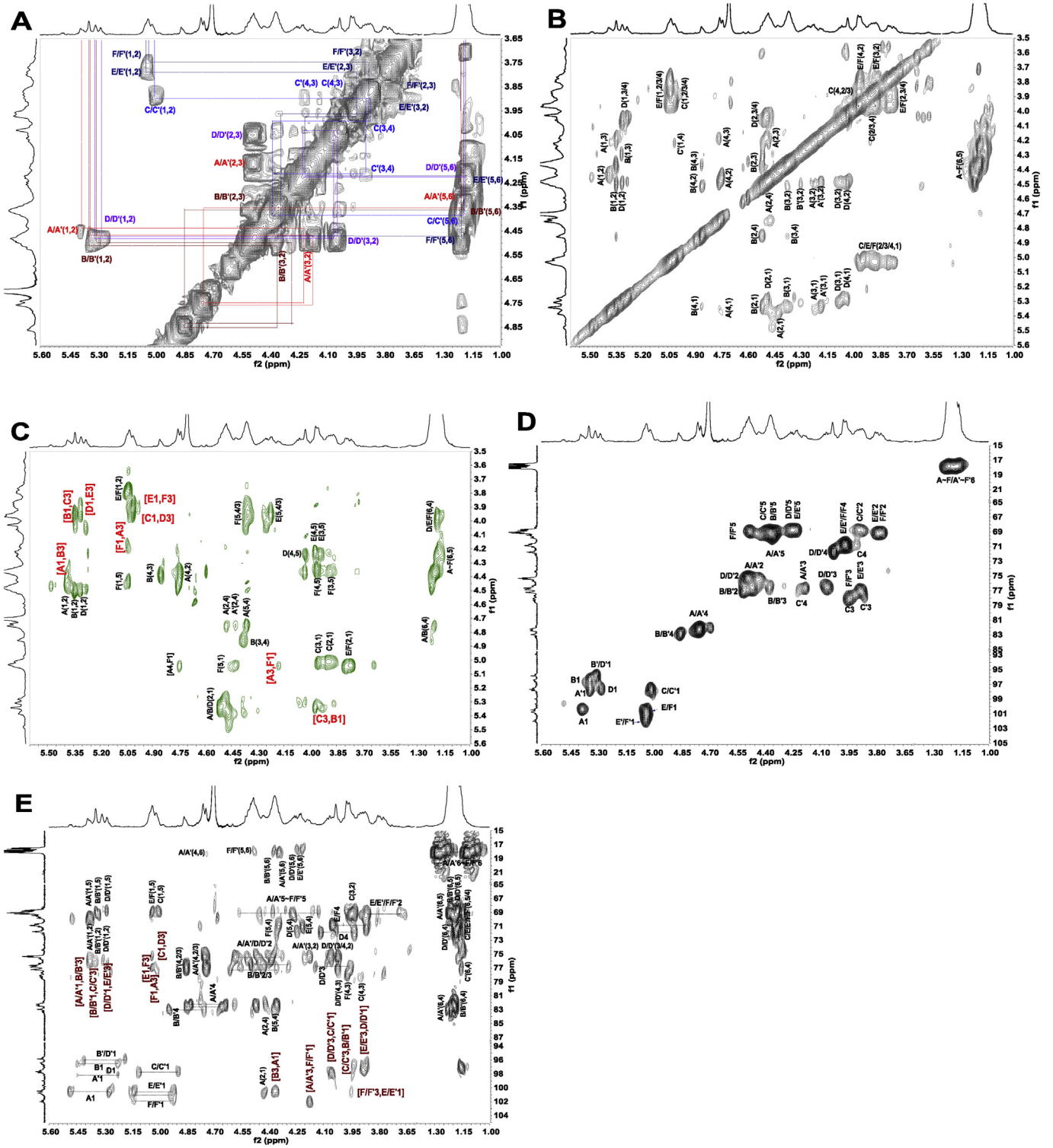

Fig. 2. Expansions of the COSY (**A**), TOCSY (**B**), ROESY (**C**), HSQC (**D**) and HMBC (**E**) spectra of the depolymerized fucan sulfate from the sea cucumber *H. albiventer*.

The order of the six residues was deduced as follow. In the 2D $^{1}H/^{1}H$ ROESY spectrum (Fig. 2C), *H*-1 of residue **A** showed cross-peak to *H*-3 of residue **B**; *H*-1 of residue B showed cross-peak to *H*-3 of residue **C**; *H*-1 of residue **C** showed cross-peak to *H*-3 of residue **D**; *H*-1 of residue **D** showed cross-peak to *H*-3 of residue **E**. Similarly, the 2D $^{13}C/^{1}H$ HMBC spectrum (Fig. 2E) also showed the sequence-defining **A**1–**B**3, **B**1–**C**3, **C**1–**D**3, **D**1–**E**3, **E**1–**F**3 and **F**1–**A**3. These evidences revealed the sequence and linkage -3-**A**-1→3-**B**-1→3-**C**-1→3-**D**-1→3-**E**-1→3-**F**-1 as the linear hexasaccharide unit as shown in Fig. 3.

To further estimate the configurations at the glycosidic linkages, the direct coupling constant ($^{1}J_{C-H}$) of *C*-1 of each monosaccharide residue was also obtained from the 2D $^{13}C/^{1}H$ HMBC spectrum (Fig. 2E). The large values of 170–175 Hz for these fucose residues indicated the protons are equatorial [34]. Taking account of the vicinal coupling constant ($^{3}J_{1H-2H}$) of 3 Hz for fucose residues, the configuration at *C*-1 of these residues was α.

Overall, the combination of chemical analysis, methylation experiments, IR and NMR spectroscopy allowed us to determine the fine

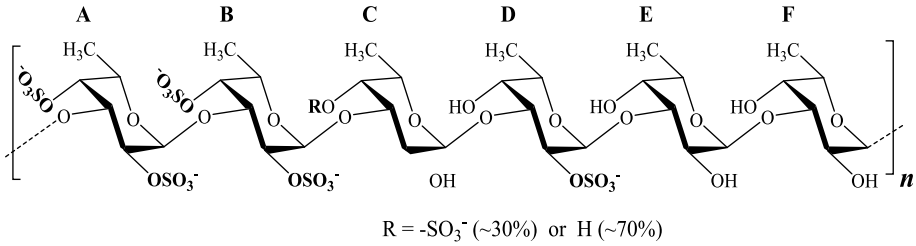

Fig. 3. Proposed structure of the fucan sulfate from the sea cucumber *H. albiventer*.

structure of the fucan sulfate from the sea cucumber *H. albiventer*. The α-*L*-fucan sulfate is essentially linear polymer, composed of regular hexasaccharide repeating units with a distinctive sulfation pattern as shown in Fig. 3.

For holothurian fucan sulfates, their specific sulfation patterns and the glycosidic linkages vary from each other, for instance, the fucan sulfates from the sea cucumbers *Isostichopus badionotus*, *Apostichopus molpadioides* and *Thelenota ananas* are all linear polysaccharides consisting of α(1 → 3) linked repetitive tetrasaccharide sequences while differ in sulfation patterns [35–37]. The body wall of sea cucumbers, *Apostichopus japonicus* (*Stichopus japonicus*) and *Holothuria edulis* contains branched polysaccharides consisting of a pentasaccharide repeating unit, which is proposed to be the major structural component of these fucan sulfates [17,32]. In this work, the *H. albiventer* fucan sulfate comprises α(1 → 3) linked repetitive hexasaccharide sequences with a specific sulfation pattern.

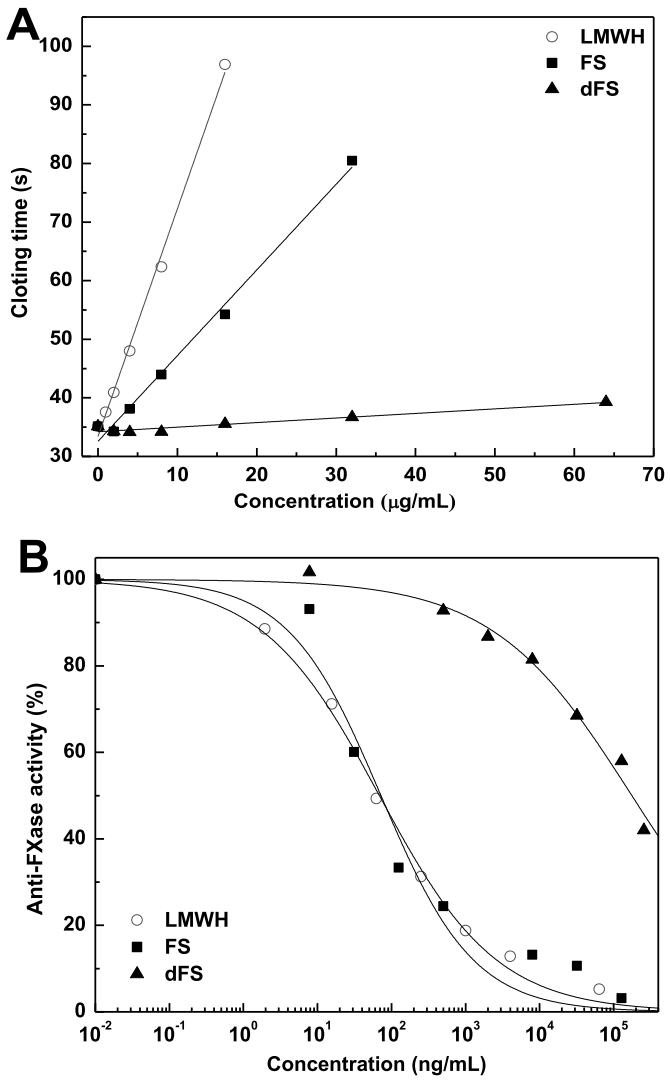

Fig. 4. Anticoagulant activities (**A**) and anti-FXase activities (**B**) of the *H. albiventer* fucan sulfate, its depolymerized product (dFS) and a low-molecular-weight heparin (LMWH).

Table 3
Anticoagulant activity and intrinsic FXase inhibitory activity of the fucan sulfate.

Sulfated polysaccharides	Mw (kDa)[a]	APTT (μg/mL)[b]	TT (μg/mL)[b]	PT (μg/mL)[b]	Anti-FXase (ng/mL)[c]
Native FS	> 2000	25.79	115.47	> 128[d]	71.99
depolymerized FS	4.33	> 128	> 128	> 128	> 100000
LMWH[e]	4.5	9.50	2.98	> 128	68.57

[a] Mw, weight average molecular weight.
[b] concentration required to double the APTT or PT or TT of human plasma.
[c] IC_{50} value, concentration required to inhibit 50% of intrinsic factor Xase.
[d] > 128, this activity was not significant at concentration as high as 128 μg/mL.
[e] LMWH, a low-molecular-weight heparin (Enoxaparin, Sanofi-Aventis, France).

2.3. Anticoagulant activity analysis

The anticoagulant activities of the new fucan sulfate and its depolymerized product (dFS) were evaluated by plasma clotting assays [38,39], including activated partial thromboplastin time (APTT), prothrombin time (PT) and thrombin time (TT) (Fig. 4, Table 3). Such assays are routinely used to determine the ability of anticoagulants to inhibit blood clotting through the intrinsic, extrinsic and common pathways of the coagulation cascade, respectively [38,40]. The concentrations of the fucan sulfate required to double the APTT and TT were 25.79 μg/mL and 115.47 μg/mL, higher than LMWH as a positive control. The results indicated that the native fucan sulfate exhibited potent anticoagulant activities by targeting the intrinsic and/or common pathway. Similar to LMWH, the native polysaccharide showed no significant PT-prolonging activity at the concentrations tested (1–128 μg/mL), indicating that this polysaccharide had no or little effect on the extrinsic coagulation pathway. However, its depolymerized product (Mw, 4.33 kDa) displayed no APTT, TT, PT-prolonging activities at the concentrations tested (1–128 μg/mL).

Since the intrinsic coagulation factor Xase complex (FXase) is the last enzyme complex that can be targeted in the intrinsic coagulation pathway [40,41], it is becoming recognized as a prime target for developing safer anticoagulants with potential physiological and therapeutic applications [42]. Thus, the intrinsic FXase inhibitory activity of the fucan sulfate and dFS was further tested (Fig. 4B, Table 3). Increasing concentrations of the sea cucumber fucan sulfate could result in essentially complete inhibition of FXase (Fig. 4B), indicating that this polysaccharide displayed a strong anti-FXase activity (IC_{50} = 71.99 ng/mL), comparable to LMWH (IC_{50} = 68.57 ng/mL). The FXase inhibitory activity of dFS was markedly lower than its native polysaccharide, indicating that anticoagulant activity of the fucan sulfate might depend on its molecular size.

3. Conclusions

In this study, we characterized the chemical structures of the fucan sulfate from the sea cucumber *H. albiventer* by chemical analysis, IR and 2D NMR spectroscopy techniques. Our data revealed that the sulfated polysaccharide is composed of regular $\alpha(1 \rightarrow 3)$ linked hexasaccharide repeating units with a distinctive sulfation pattern. Anticoagulant assays indicated that the fucan sulfate possessed strong APTT and TT prolonging activities and intrinsic factor Xase inhibitory activity. The *in vitro* data encourage a much more detailed screening of the *in vivo* anticoagulant and antithrombotic effects of the well-defined fucan sulfate.

4. Experimental

4.1. Materials

Dried sea cucumber *H. albiventer* was purchased in seafood markets in Guangzhou city of Guangdong province (China). Amberlite FPA98Cl ion exchange resin was purchased from Rohm and Haas Company (USA). The monosaccharide standards including *D*-glucuronic acid (GlcA), *D*-glucose (Glc), *D*-galactose (Gal) and *D*-mannose (Man) were purchased from Alfa Aesar. *L*-rhamnose (Rha) was purchased from TCI. *L*-fucose (Fuc) and 1-phenyl-3-methyl-5-pyrazolone (PMP, 99%) were purchased from Sigma Chemical Co. (Shanghai, China). LMWH (Enoxaparin, 0.4 mL × 4000 AXaIU) was from Sanofi-Aventis (France). The activated partial thromboplastin time (APTT), prothrombin time (PT), thrombin time (TT) reagents, and standard human plasma were from Teco Medical (Germany). Biophen FVIII: C kit was from Hyphen Biomed (France). Human factor VIII was from Bayer HealthCare LLC (Germany). All of other chemicals and reagents were of commercially available analytical grade.

4.2. Extraction and purification of the polysaccharide

The crude polysaccharides were extracted from the milled body wall of the sea cucumber *H. albiventer* according to the method in our previous reports with minor modifications [16,19,20]. The powder of 300 g dried body wall of *H. albiventer* was mixed up with 3 L of deionized water containing 3 g papain and incubated at 50 °C for 6 h. The resulting mixture was diluted with 600 mL of 1.5 M sodium hydroxide and reacted at 50 °C for 2 h. After the reactant solution was adjusted to pH 7 and centrifuged at 3000 × g for 20 min, the supernatant was precipitated by adding ethanol to a final concentration of 60% (v/v) to obtain the crude polysaccharides The crude polysaccharide was dissolved with 2 L of distilled water containing 67 mL of 30% H_2O_2 and decolorized at pH 10 and 45 °C for 3 h. After adjusted pH to 7 and centrifuged, the solution was precipitated by adding potassium acetate to a final concentration of 1 M and ethanol to 40% (v/v). The resulting precipitate was mainly the crude fucosylated chondroitin sulfate, and the supernatant was further precipitated with ethanol at 60% (v/v). After centrifugation, the crude fucan sulfate was obtained with the yield of 4.17%.

The crude fucan sulfate was further purified using strong anion exchange chromatography on a FPA98 column (5 cm × 50 cm). The purity and the average molecular weight were analyzed by high-performance gel permeation chromatography (HPGPC) using an Agilent technologies1200 series (Agilent Co., USA) apparatus with RID detector, equipped with a Shodex OH-pak SB-806 HQ column (8 mm × 300 mm) and eluted with 0.1 M NaCl (35 °C, 0.5 mL/min).

4.3. Monosaccharide composition analysis

The monosaccharide composition of the polysaccharide was analyzed by reverse-phase HPLC after PMP pre-column derivatization procedures [17,21,22]. The polysaccharide and standard monosaccharides were respectively hydrolyzed with trifluoroacetic acid, and evaporated to dryness. The dry samples were dissolved and reacted with PMP in methanol under the alkaline condition, to prepare the monosaccharide derivatives of PMP for HPLC analysis. The chromatographic conditions were performed according to the previous method [17,21].

The sulfate contents of the polysaccharides were measured by conductometric method [24]. The acid form of samples was prepared using the strong acidic cation exchange resin with Dowex R 50w × 8 50–100H and titrated by a strong base titration solution of 0.2 M NaOH to record the conductivity value, then the sulfate content and the molar ratio were calculated by the conductance curve.

4.4. Methylation analysis

Methylation experiment of the polysaccharide was performed according to the literature [17,21]. The native fucan sulfate was dissolved in dimethyl sulfoxide and methylated using methyl iodide by ultrasonic reaction. Then, the methylated polysaccharide was hydrolyzed with trifluoroacetic acid, reduced by sodium borodeuteride, and the resulting alditols were acetylated by pyridine and acetic anhydride. Finally, the alditol acetates were detected by GC–MS by a previously reported method [21].

4.5. Preparation of the desulfated product

Desulfuration of the native polysaccharide were carried out according to the method with minor modifications [43]. The acid resolution of about 80 mg fucan sulfate was prepared using the strong acidic cation exchange resin with Dowex R 50w × 8 50–100H, neutralized with pyridine and lyophilized. The pyridinium salt was dissolved in 8 mL dimethylsulfoxide/methanol (9: 1, v/v), heated at 80 °C for 9 h, dialyzed by a dialysis bag with a molecular weight cutoff of 1 kDa and lyophilized to obtain the desulfated product with the yield of 23.9%.

4.6. Preparation of the depolymerized fucan sulfate

In order to further confirm the structure of the native fucan sulfate, its depolymerized product (4.33 kDa) was prepared according to an established method with some modifications [26]. The polysaccharide (209.5 mg) and copper sulfate (1.27 mg) were dissolved in 8 mL of deionized water, then the mixture was reacted with 1.56 mL of 10% H_2O_2 at 35 °C for 7 h. After added 2 mL of saturated sodium chloride solution, the solution was precipitated by adding ethanol to a final concentration of 80% (v/v). Then, the precipitate was collected by centrifugation, dissolved in water, dialyzed by a dialysis bag with a molecular weight cutoff of 1 kDa, and lyophilized to obtain the depolymerized product (dFS). The yield of dFS was 46.1%. Its physicochemical characteristics were analyzed, containing sulfate content, specific rotation and infrared spectroscopy. The chemical structure was further deduced by 1D/2D NMR analysis.

4.7. Spectrometry analysis

Infrared Spectroscopy was recorded using a Fourier transform IR spectrophotometer (Nicolet Is10, Thermo). The mixture of the native fucan sulfate or the depolymerized product and KBr was ground to powder, and pressed into pellets for IR spectral measurement in the frequency range of 400–4000 cm^{-1} at room temperature.

One-dimensional spectra ($^1H/^{13}C$ NMR) and Two-dimensional spectra (COSY, TOCSY, ROESY, HSQC and HMBC) were acquired at 298 K on a 600/800 MHz Bruker Avance spectrometer with HOD suppression by pre-saturation as previously described [38,40]. All samples were previously dissolved in deuterium oxide (D_2O, 99.9% D) and lyophilized three times to replace exchangeable protons with D_2O. All

chemical shifts were relative to internal trimethylsilyl-propionic acid (TSP).

4.8. Biological activity assays

The activated partial thromboplastin time (APTT), prothrombin time (PT) and thrombin time (TT) were measured using APTT, PT and TT assay kits and standard human plasma on a coagulometer (TECO MC-4000, Germany), as previously described [38,39]. The activity of intrinsic factor Xase complex inhibition was detected using the BIOPHEN FVIII: C kit by a Bio-Tek microplate reader (Amecrica) according to the previously described method [38,39].

Conflicts of interest

The authors declare no conflicts of interest.

Acknowledgments

This work was funded in part by the National Natural Science Foundation of China (81673330, 81703374, and 81773737), Yunnan Provincial Science and Technology Department in China (2016FA050 and 2014FB078), a grant from Youth Innovation Promotion Association (2017435), Kunming Institute of Botany (KIB2017011), Discovery, Evaluation and Transformation of Active Natural Compounds, Strategic Biological Resources Service Network Programme (ZSTH-020) of Chinese Academy of Sciences.

Appendix A. Supplementary data

Supplementary data related to this article can be found at http://dx.doi.org/10.1016/j.carres.2018.05.007.

References

[1] M.B. Streiff, P.L. Bockenstedt, S.R. Cataland, C. Chesney, C. Eby, J. Fanikos, P.F. Fogarty, S. Gao, J. Garcia-Aguilar, S.Z. Goldhaber, H. Hassoun, P. Hendrie, B. Holmstrom, K.A. Jones, N. Kuderer, J.T. Lee, M.M. Millenson, A.T. Neff, T.L. Ortel, J.L. Smith, G.C. Yee, A. Zakarija, J. Natl. Compr. Canc. Netw. 9 (2011) 714–777.
[2] D.L. Rabenstein, Nat. Prod. Rep. 19 (2002) 312–331.
[3] L. Fu, M. Suflita, R.J. Linhardt, Adv. Drug Deliv. Rev. 97 (2016) 237–249.
[4] P.A. Mourão, M.S. Pereira, Trends Cardiovasc. Med. 9 (1999) 225–232.
[5] H.A.O. Rocha, F.A. Moraes, E.S. Trindade, C.R.C. Franco, R.J.S. Torquato, S.S. Veiga, A.P. Valente, P.A.S. Mourão, E.L. Leite, H.B. Nader, C.P. Dietrich, J. Biol. Chem. 280 (2005) 41278–41288.
[6] P.A.S. Mourão, Curr. Pharm. Des 10 (2004) 967–981.
[7] V.H. Pomin, M.S. Pereira, A.P. Valente, D.M. Tollefsen, M.S.G. Pavao, P.A.S. Mourão, Glycobiology 15 (2005) 369–381.
[8] M.I. Bilan, A.A. Grachev, A.S. Shashkov, M. Kelly, C.J. Sanderson, N.E. Nifantiev, A.I. Usov, Carbohydr. Res. 345 (2010) 2038–2047.
[9] E. Deniaud-Bouët, K. Hardouin, P. Potin, B. Kloareg, C. Hervé, Carbohydr. Polym. 175 (2017) 395–408.
[10] O. Berteau, B. Mulloy, Glycobiology 13 (2003) 29r–40r.
[11] A.D. Holtkamp, S. Kelly, R. Ulber, S. Lang, Appl. Microbiol. Biotechnol. 82 (2009) 1–11.
[12] Y.G. Chang, Y.F. Hu, L. Yu, D.J. McClements, X.Q. Xu, G.C. Liu, C.H. Xue, Carbohydr. Polym. 136 (2016) 1091–1097.
[13] V.H. Pomin, Biopolymers 91 (2009) 601–609.
[14] B. Mulloy, A.C. Ribeiro, A.P. Alves, R.P. Vieira, P.A.S. Mourão, J. Biol. Chem. 269 (1994) 22113–22123.
[15] M.S. Pereira, B. Mulloy, P.A.S. Mourão, J. Biol. Chem. 274 (1999) 7656–7667.
[16] L. Luo, M. Wu, L. Xu, W. Lian, J. Xiang, F. Lu, N. Gao, C. Xiao, S. Wang, J. Zhao, Mar. Drugs 11 (2013) 399–417.
[17] M. Wu, L. Xu, L. Zhao, C. Xiao, N. Gao, L. Luo, L. Yang, Z. Li, L. Chen, J. Zhao, Mar. Drugs 13 (2015) 2063–2084.
[18] N.E. Ustyuzhanina, M.I. Bilan, A.S. Dmitrenok, E.Y. Borodina, N.E. Nifantiev, A.I. Usov, Carbohydr. Res. 456 (2018) 5–9.
[19] X. Li, L. Luo, Y. Cai, W. Yang, L. Lin, Z. Li, N. Gao, S.W. Purcell, M. Wu, J. Zhao, J. Agric. Food Chem. 65 (2017) 9315–9323.
[20] F. Shang, R. Mou, Z. Zhang, N. Gao, L. Lin, Z. Li, M. Wu, J. Zhao, Carbohydr. Polym. 195 (2018) 257–266.
[21] J. Liu, F. Shang, Z. Yang, M. Wu, J. Zhao, Int. J. Biol. Macromol. 98 (2017) 786–792.
[22] J. Liu, L. Zhou, Z. He, N. Gao, F. Shang, J. Xu, Z. Li, Z. Yang, M. Wu, J. Zhao, Carbohydr. Polym. 181 (2018) 433–441.
[23] M.I. Bilan, A.A. Grachev, N.E. Ustuzhanina, A.S. Shashkov, N.E. Nifantiev, A.I. Usov, Carbohydr. Res. 339 (2004) 511–517.
[24] B. Casu, U. Gennaro, Carbohydr. Res. 39 (1975) 168–176.
[25] I.M. Sims, S.M. Carnachan, T.J. Bell, S. Hinkley, Carbohydr. Polym. 188 (2018) 1–7.
[26] M. Wu, S. Xu, J. Zhao, H. Kang, H. Ding, Food Chem. 122 (2010) 716–723.
[27] B. Matsuhiro, Hydrobiologia 327 (1996) 481–489.
[28] B. Matsuhiro, I.O. Osorio-Román, R. Torres, Carbohydr. Polym. 88 (2012) 959–965.
[29] N.P. Chandía, B. Matsuhiro, Int. J. Biol. Macromol. 42 (2008) 235–240.
[30] W. Jin, Z. Guo, J. Wang, W. Zhang, Q. Zhang, Carbohydr. Res. 369 (2013) 63–67.
[31] M.I. Bilan, A.A. Grachev, A.S. Shashkov, T.T. Thuy, T.T. Van, B.M. Ly, N.E. Nifantiev, A.I. Usov, Carbohydr. Res. 377 (2013) 48–57.
[32] P.A. Mourão, E. Vilanova, P.A. Soares, Curr. Opin. Struct. Biol. 50 (2018) 33–41.
[33] M. Wu, R. Huang, D. Wen, N. Gao, J. He, Z. Li, J. Zhao, Carbohydr. Polym. 87 (2012) 862–868.
[34] K. Yoshida, Y. Minami, H. Nemoto, K. Numata, E. Yamanaka, Tetrahedron Lett. 33 (1992) 4959–4962.
[35] S. Chen, Y. Hu, X. Ye, G. Li, G. Yu, C. Xue, W. Chai, Biochim. Biophys. Acta 1820 (2012) 989–1000.
[36] L. Yu, C. Xue, Y. Chang, X. Xu, L. Ge, G. Liu, Y. Wang, Food Chem. 146 (2014) 113–119.
[37] L. Yu, L. Ge, C. Xue, Y. Chang, C. Zhang, X. Xu, Y. Wang, Food Chem. 142 (2014) 197–200.
[38] F. Shang, N. Gao, R. Yin, L. Lin, C. Xiao, L. Zhou, Z. Li, S.W. Purcell, M. Wu, J. Zhao, Eur. J. Med. Chem. 148 (2018) 423–435.
[39] M. Wu, D. Wen, N. Gao, C. Xiao, L. Yang, L. Xu, W. Lian, W. Peng, J. Jiang, J. Zhao, Eur. J. Med. Chem. 92 (2015) 257–269.
[40] L. Zhao, M. Wu, C. Xiao, L. Yang, L. Zhou, N. Gao, Z. Li, J. Chen, J. Chen, J. Liu, H. Qin, J. Zhao, Proc. Natl. Acad. Sci. U. S. A 112 (2015) 8284–8289.
[41] J.P. Sheehan, E.N. Walke, Blood 107 (2006) 3876–3882.
[42] Y. Buyue, J.P. Sheehan, Blood 114 (2009) 3092–3100.
[43] P.A.S. Mourão, A.S. Perlin, Eur. J. Biochem. 166 (1987) 431–436.